Application of Actuators to Control Beam Flexure in a Large Space Structure

Shalom Fisher*
Naval Research Laboratory, Washington, D.C.

This paper describes a flexible-body control methodology for performing a nonlinear slew of a large space structure and simultaneously regulating the associated flexural vibrations by linear methods. Degree of controllability methods are used as guidelines for the positioning of proof-mass actuators on the structure. The goal is to determine the importance of location of the actuators on regulator performance, and the utility of the degree of controllability methods. A numerical simulation is made of a 20 deg slew maneuver of the spacecraft laboratory experiment (SCOLE). The SCOLE model treated here is the spacecraft version. It includes three bodies: the Space Shuttle, a reflector antenna, and a flexible beam of length 39.62 m connecting them. In the simulation, the beam vibration is fully coupled to the dynamics of the slewing motion. Regulation of the beam vibration is addressed by means of proof-mass actuators on the beam, and by vernier thrusters on the Shuttle and antenna bodies. Repeated simulations are made with different actuator placements. The results show that with the actuators placed within a region of strong control effectiveness, damping and flexural amplitude are changed only slightly by changes in actuator location. However, the damping is significantly reduced for actuator location in regions of low-control effectiveness, although the amplitude of the vibrations changes only slightly.

Introduction

THE methodology for control of a large-angle slew, described in this paper, was originally conceived as a response to the design challenge of Taylor and Balakrishnan.[1] In the design challenge, the Spacecraft Laboratory Experiment (SCOLE) project was set up by NASA Langley Research Center to provide a standard configuration to test control laws. The SCOLE project includes a mathematical model of a spacecraft and a laboratory apparatus. The laboratory apparatus has been constructed at NASA Langley and is available for investigators.[2] The spacecraft model includes the Space Shuttle connected by a long (130 ft, 39.62 m) flexible beam to a hexagonal antenna or reflector, as shown in Fig. 1. The reflector and Shuttle are treated as rigid bodies. In the configuration, the line-of-sight (LOS) vector is defined as the direction of a signal emitted from a point in the cargo bay located 1.143 m (3.75 ft) in front of the base of the beam, and reflected off the center of the reflector in the direction of a distant target. The primary design challenge presented by Taylor and Balakrishnan[1] is to develop control laws to rapidly slew the LOS through 20 deg and to damp the structural vibrations to a residual pointing error of less than 0.02 deg. The torque needed to perform the slew is provided by thrusters of 13,558 N-m (10,000 ft-lb) capacity acting about each axis of the Shuttle and on the reflector, and by control forces on the center of the reflector, which have a maximum thrust of 3558.6 N (800 lb). Two pairs of proof-mass actuators with capacity 44.48 N (10 lb) along each orthogonal axis are available to be positioned at arbitrary points on the beam to regulate the slew maneuver and to damp the vibrations. Control of the end points of the beam is achieved by fine tuning the thrusters on the Shuttle body and reflector.

Work on the SCOLE concept has been performed by a number of investigators. Some of the results of this work have been reported at the SCOLE workshops[3] at NASA Langley Research Center, Dec. 6-7, 1984, Dec. 9-10, 1985, and Nov. 17-18, 1986, and at the U.S. Air Force Academy, Nov. 16, 1987. A number of investigators have addressed the specific question of the development of control laws for performing the slewing maneuver and damping the vibrations in both the laboratory apparatus and the mathematical model versions of the SCOLE configuration. Meirovitch and Quinn[4,5] have reported on a number of different aspects of the problem, including control law design for both of the models. Their method decouples the problem of maneuver control from the problem of vibration control by means of the assumption of linear elastic displacements. The difference between their work and the work to be described in this paper is that here we assess the sensitivity of the vibrational amplitude and damping to changes in the location of the proof-mass actuators. Norris et al.[6] use component cost analysis to find that the best place for location of the proof-mass actuators is near the top of the beam for both pairs of actuators. It is not clear whether or not they include the control moments, provided by thrusters, that can be applied to the antenna and the Shuttle body. They do not simulate an actual slew, as is done in the present investigation. Lin[7] has looked at modal dashpot and modal spring control of flexure vibrations. He has determined the line-of-sight pointing error due to each mode individually, and thereby has assessed the relative importance of each mode. Kakad[8,9] expresses the rotational and vibration equations in terms of Euler parameters and modal coordinates. He develops a set of dynamic equations describing the slewing maneuver in terms of a distributed parameter model for the beam. His analysis shows that mode coupling generates serious control spillover from the higher uncontrolled modes. Bainum and Li[10] discuss a number of issues governing the development of control strategies for performing the slew maneuver and damping, and develop stability criteria for maximum time lag in actuator response.

Received Sept. 28, 1987; revision received April 4, 1988.

*Research Physicist, Naval Center for Space Technology.

Numerical Algorithms Used in the Simulation

The nonlinear slew maneuver of the SCOLE system is simulated with the Dynamic Interaction Simulation of Controls and

Structure (DISCOS) program.[11] DISCOS requires specification of the number and type (whether rigid or flexible) of bodies in the system. The magnitude of the masses and moments of inertia of the bodies in the system as well as the magnitude and direction of externally applied forces and torques are also user-specified. Table 1 gives the system data used in this simulation.

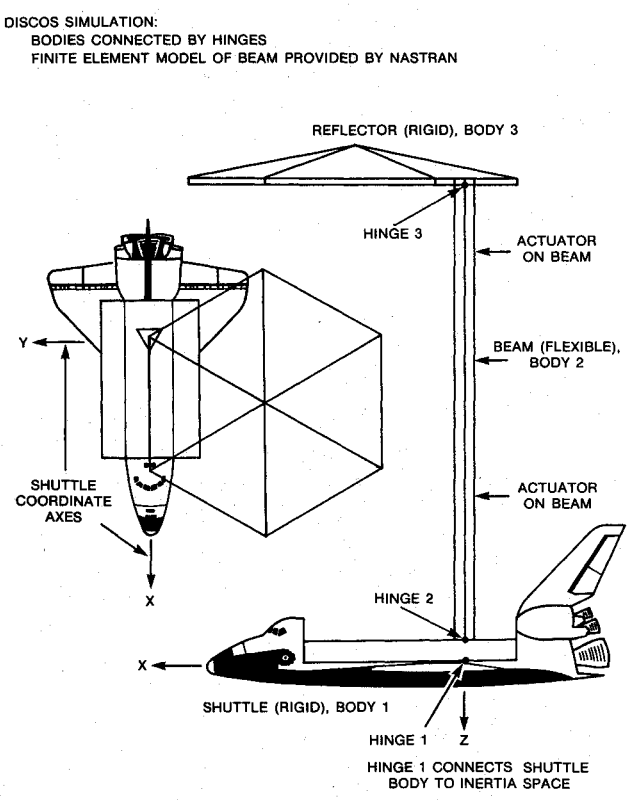

Fig. 1 SCOLE configuration showing the three-body model, coordinate system, and actuator control points.

Each body must have at least one "hinge" with up to 6 degrees of freedom, by which it is attached to other bodies. An additional hinge is required to attach body one, in this case the Shuttle body, to inertial space.

The DISCOS program requires an initial calculation, performed externally, of the free vibration modal frequencies (or modal mass and stiffness), damping, and eigenvectors for each flexible body. It should be noted that the vibration amplitudes and rates of change of the amplitudes, assumed to be linear, are fully coupled to the dynamical motion of the bodies in this system during the simulation. Here, the eigenvectors are calculated by means of a NASTRAN finite-element program.[12] The Euler-Bernoulli equations are solved for a force-free beam with free-free boundary conditions.[13] We use an augmented body method[14] to obtain eigenfrequencies that are close to the linear force-free vibrations of the entire SCOLE system. In this method, the beam is modeled as a structure that contains the beam plus end regions. Each end region is mass-loaded with the mass and inertia properties of the attached body. The beam itself is divided into 21 equally spaced nodal points. A lumped mass approximation is used, with each interior nodal point assigned 1/20 of the beam mass, and 1/20 of the transverse moments of inertia, I_{xx} and I_{yy}. Half-values of mass and inertia moments are assigned to each of the two exterior points. The eigenvectors and modal frequencies are then derived by assuming that the entire beam structure, including the end regions, can vibrate freely. We keep only the 12 lowest modes for the DISCOS simulation because of computer time limitations.

The displacement of the kth eigenvector at the point j is a vector with three spatial and three rotational components, denoted as

$$\phi_j^{(k)} = (\phi_{\theta x},\phi_{\theta y},\phi_{\theta z},\theta_x,\phi_y,\phi_z)_j^{(k)}, \qquad \begin{matrix} i = 1,2,...21 \\ k = 1,2,...12 \end{matrix} \quad (1)$$

Here, $\phi_{\theta x},\phi_{\theta y},\phi_{\theta z}$ are the modal rotations about the x, y, and z axes, and ϕ_x,ϕ_y,ϕ_z are the modal displacements along the x, y, and z axes. From the eigenvectors, it is possible to identify the principal orientation of the modes, i.e., whether a given mode

Table 1 Physical characteristics of SCOLE spacecraft model, including applied forces and torques

Forces and Torque	Symbol	Value
Force at top of reflector	F_y	40 N(9 lb)[a]
Torque at reflector	T_x	236 N-m(174 ft-lb)
Torques on Shuttle body	T_x	13,558 N-M(10,000 ft-lb)
	T_z	−2300 N-m(−1700 ft-lb)

Masses and moments of inertia of system and component

Body	Mass, kg (lb)	I_{xx} kg-m^2 (slug-ft^2)	I_{yy}	I_{zz}	I_{xy}	I_{xz}	I_{yz}
Antenna (reflector)	181.52	6.737 E3[b]	6.737 E3	1.347 E4	0	0	0
CG	(400)	(4.969 E3)	(4.969 E3)	(9.938 E3)			
Antenna (reflector)	181.52	2.440 E4	1.266 E4	3.715 E4	−1.026 E4	0	0
attachment point	(400)	(1.800 E4)	(9.336 E3)	(2.471 E4)	(−7.57 E3)		
Shuttle body	9.303 E4	1.228 E6	9.205 E6	9.608 E6	0	1.971 E5	0
	(2.050 E5)	(9.054 E5)	(6.789 E6)	(7.087 E6)		(1.454 E5)	
System minimum principal moment of inertia I_1		1.268 E6	(1.201 E6)				

Boom properties
Mass = 181.52 kg (400 lb)
Area moments of inertia, $I_{xx} = I_{yy} = 2.40$ E − 3 m^4(0.278 ft^4)
Torsional constant, $J = 6.14$ E − 4 m^4 (0.883 ft^4)
Cross section, $A = 6.955$ E − 4 m^2(7.486 E-3 ft^2)
Elasticity, $E = 6.89$ E10 Pa(1.439 E10 lbf/ft^2, 1.0 E7 lbf/in^2.)

[a]Units are in MKS with English units in parentheses; [b]E means 10 to the power of.

Table 2 Locations of nodal points on mast, mode numbers, types, and frequencies

Node no.	Distance from Shuttle, m (ft)	Mode no.	Mode type	Angular frequency	Frequency, Hz
1–7	On reflector body	1	Pitch	1.746	0.278
8	39.624 (130.0)	2	Roll	1.969	0.313
9	37.643 (123.5)	3	Yaw	5.105	0.812
10	35.662 (117.0)	4	Roll	7.410	1.179
11	33.680 (110.5)	5	Pitch	12.848	2.045
12	31.699 (104.0)	6	Roll	29.459	4.689
13	29.718 (97.5)	7	Pitch	34.263	5.453
14	27.737 (91.0)	8	Roll	74.670	11.884
15	25.756 (84.5)	9	Pitch	78.883	12.555
16	23.774 (78.0)	10	Compression	106.281	16.915
17	21.793 (71.5)	11	Roll	142.467	22.674
18	19.812 (65.0)	12	Pitch	145.618	23.176
19	17.831 (58.5)				
20	15.850 (52.0)				
21	13.868 (45.5)				
22	11.887 (39.0)				
23	9.906 (32.5)				
24	7.925 (26.0)				
25	5.944 (19.5)				
26	3.962 (13.0)				
27	1.981 (6.5)				
28	0 (0.0)				
29–40	On Shuttle body				

is a roll, pitch, yaw, or a compression of the beam. Of course, each mode has nonzero components about all three axes. The frequency and principal orientation of the 12 lowest modes are given in Table 2. Figure 2 shows the modal displacements in roll as a function of distance along the beam with the Shuttle end at zero and the reflector at 130. Each mode is separately normalized.

Formulation of Control Law for the Nonlinear Slew Maneuver

The control law for performing the time-optimal slew of the SCOLE configuration is formulated with a rigid-body model of the system, even though the actual simulation assumes flexibility in the beam. The slew is constrained to proceed about the minimum axis of inertia of the system. The goal is to apply a control torque $T(t)$ to minimize the performance index

$$J(t_0) = \min \int_{t_0}^{t_f} \mathrm{d}t \tag{2}$$

subject to

$$I_1 \ddot{\theta}_1(t) = T(t) \tag{3}$$

$$\dot{\theta}_1(t_0) = \dot{\theta}_1(t_f) = 0 \tag{4}$$

$$\theta_1(t_0) = 20 \text{ deg}, \qquad \theta_1(t_f) = 0 \tag{5}$$

$$|T(t)| \leq T_{\max} \tag{6}$$

Here, I_1 is the minimum moment of inertia of the system, θ_1 the angle of rotation about the minimum inertia axis, $T(t)$ the applied torque, t_0 the initial time, and t_f the final time to be minimized. Equation (3) is Euler's equation for a rigid body. There is assumed to be no angular momentum about the other two principal axes and, therefore, no cross-coupling terms appear in Eq. (3). Since the minimum inertia axis is nearly aligned with the roll axis of the Shuttle body, the principal torque is about that axis. The values of the forces and torques used in this simulation are given at the top of Table 1.

The solution to Eqs. (2–6) can be found in any standard work on optimal control. It is well known that the optimal solution is a bang-bang control policy.[15] For the rigid-body slew, the switching time will be given by

$$t_s = \sqrt{[I_1 \theta_1(t_0)/T_{\max}]} \tag{7}$$

In this calculation, $t_s = 5.65$ s, with a cutoff time of $2^* t_s = 11.30$ s for completion of the slew.

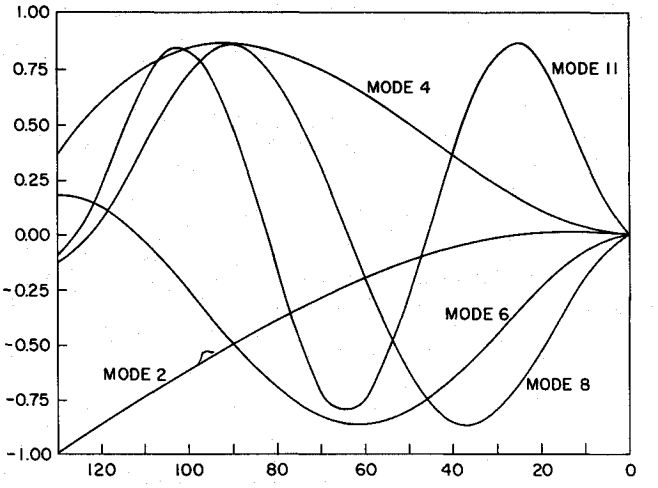

Fig. 2 Roll modes: normalized modal displacements in Y as a function of distance in feet from Shuttle body.

Regulator Control-Law Development using Linear Quadratic Regulator (LQR) Methods

The development of the regulator to minimize beam flexure during the slew begins with the linear system equations with external forces:

$$\{\dot{x}(t)\} = [A]\{x(t)\} + [B]\{u(t)\} \tag{8}$$

In the 24 component vector $\{\dot{x}(t)\}$, the first 12 components contain the modal velocities $\{\dot{\xi}\}$ followed by the 12 modal

displacements $\{\xi\}$. The matrix $[A]$ is given by

$$[A] = \begin{bmatrix} 0 & -[\omega^2] \\ [I_{12}] & 0 \end{bmatrix} \tag{9}$$

where $[\omega^2]$ is a 12×12 diagonal matrix of modal frequencies, and $[I_{12}]$ the unit matrix of dimension 12. The input vector $\{u\}$ is the length 24, since each of the four points of control on the beam has 6 degrees of freedom. the points are arranged with points 1 and 4 at the attachment points of the beam to the antenna and Shuttle, respectively; points 2 and 3 are at intermediate locations on the beam. The vector $\{u\}$ is structured such that the elements are of the form

$u_1 = \tau_{1\theta x}$ (torque at point 1 about x axis)

$u_4 = f_{1x}$ (force at point 1 in x direction)

$u_7 = \tau_{2\theta x}$ (torque at point 2 about x axis), etc.

Many of the elements of $\{u(t)\}$ are zero in the simulation due to limitations on the control forces. At points 2 and 3, for example, only forces in x and y directions provide nonzero elements to $\{u(t)\}$. The 24×24 control distribution matrix $[B]$ is derived from the set of mode shape functions. The first 12 rows of $[B]$ are structured as follows:

$$(B)_k = [\phi_1^{(k)}, \phi_2^{(k)}, \phi_3^{(k)}, \phi_4^{(k)}] \tag{10}$$

where the $\phi_j^{(k)}$ are defined in Eq. (1). The last 12 rows of $[B]$ are zero. It should be noted that the control points are at nodal points.

The deterministic LQR methods minimize a cost functional J where we have

$$J = \int_0^\infty \left(\{x(t)\}^T [Q] \{x(t)\} + \{u(t)\}^T [R] \{u(t)\} \right) \mathrm{d}t, \tag{11}$$

where the superscript T means transpose of the vector or matrix. Here, $[Q]$ and $[R]$ are weighting matrices that are used in the minimization of J to balance the two conflicting objectives of maximizing the system performance without the control effort getting too large. The additional constraint of the 44.48 N force limitation on the proof-mass actuator control effort is incorporated in the simulation by switching off the actuator if the limit is exceeded.

For simplicity in this analysis, $[Q]$ is chosen to be the unit matrix $[I_{24}]$, with $[R]$ set equal to $r^*[I_{24}]$. The parameter r is varied between 10^{-5} and 5^*10^{-7}. The minimization of J leads to the control algebraic Riccati equation (CARE) for the matrix $[P]$:

$$0 = [Q] + [A]^T[P] + [P][A] - [P][B][R]^{-1}[B]^T[P] \tag{12}$$

From the solution $[P]$ the input force vector $\{u(t)\}$ is given by

$$\{u(t)\} = -[R]^{-1}[B]^T[P]\{x(t)\} \tag{13}$$

In the DISCOS simulation of the slew, $\{u(t)\}$ is recalculated at each time step from the current values of $\{x(t)\}$. The regulator is in this manner fully incorporated into the beam flexure and dynamics of the slewing motion.

With the 0.01 s time step used in the simulation, four time steps cover the period of the fastest mode treated, 23.2 Hz. As a check to assess time step effects, a test run was made with a time step of 0.001 s. Since no difference in beam flexure was observed, the time step of 0.01 s appears to have been adequate.

Actuator Placement Strategies

The actuator placement strategies used in this analysis are based on the concept of "degree of controllability" as defined by Viswanathan et al.[16] In their work, they refer to a "recovery region" defined in the state space $\{x(t)\}$. For our purposes, this recovery region is the set of flexure amplitudes from which bounded actuator control forces can still, but just barely, return the beam to a straight position within a given time T. Each pair of actuator placement points has a different set of such flexure amplitudes, or recovery region. A scalar measure of the size of this recovery region for each time T and for a normalized control effort is the basis by which the time-optimal degree of controllability is defined. An approximate formula for this degree of controllability ρ_{ij} is derived from a formula given by Lindberg[17] as

$$\rho_{ij} = \min_k [(\varepsilon^*(|\phi_i^{(k)}| + |\phi_j^{(k)}|) + |\phi_1^{(k)}| + |\phi_{21}^{(k)}|)/N_k^*\omega_k] \tag{14}$$

where the minimization over k covers the set of 12 modes. The level of control effort has been normalized to unity. The time T is a parameter that is suppressed, since our purpose is to compare actuator locations, with other factors being equal. The i and the j refer to arbitrary nodal point locations on the beam reflecting the influence of the two proof-mass actuator pairs. The 1 and 21 reflect the influence of the control forces at the beam ends where the Shuttle and reflector are attached. The absolute values of the modal displacements $\phi_j^{(k)}$ are obtained from Eq. (1). At the points i or j we have

$$|\phi_j^{(k)}| = |(\phi_x)_j^{(k)}| + |(\phi_y)_j^{(k)}| \tag{15}$$

since the proof-mass actuator pairs operate in the x and y directions. At the nodal point 1 (Shuttle) we have

$$|\phi_1^{(k)}| = |\phi_{\theta x1}^{(k)}| + |\phi_{\theta y1}^{(k)}| + |\phi_{\theta z1}^{(k)}| \tag{16}$$

since control torques can be applied about all three axes. The $|\phi_{21}^{(k)}|$ at the reflector attachment point includes the absolute values of the rotational modal displacements and the modal displacements in x and y. The parameter N_k is a weighting factor applied to mode k; ω_k is the characteristic frequency of mode k. The weighting used in this analysis is

$$N_i/N_j = \omega_j/\omega_i$$

which reflects the expectation that the contribution of a mode to the size of the recovery region is inversely proportional to the modal frequency. The parameter ε determines the relative weighting of the influence toward controlling flexure of the proof-mass actuators located on the beam to that of the torque thrusters located on the reflector and Shuttle bodies.

The problem of where to place the actuators on the beam is addressed by calculating the maximum value of ρ_{ij}. Five calculations of the ρ_{ij} array are made as follows: 1) $\varepsilon = 0.01$, 2) $\varepsilon = 0.1$, 3) $\varepsilon = 1$, 4) $\varepsilon = 10$, 5) $\varepsilon = \infty$ (no thrusters). The control points that give the maximum ρ_{ij} are: Case 1, $i = 16$, $j = 16$; Case 2, $i = 13$, $j = 17$; Case 3, $i = 14$, $j = 17$; Case 4, $i = 11$, $j = 16$; and Case 5, $i = 11$, $j = 16$.

Regulator Effectiveness during Nonlinear Slew Simulation

The regulator performance is described in terms of the relative roll $\Delta\theta$, the relative pitch $\Delta\phi$, and the relative yaw $\Delta\psi$ between the reflector and Shuttle body. We define Σ as the sum of the absolute values of $\Delta\theta$, $\Delta\phi$, and $\Delta\psi$; it thereby gives approximately 0.5 the LOS pointing error due to flexure. There are three significant aspects of Σ: the maximum Σ, the average Σ, and the time required after completion of the slew for Σ to settle down below 0.01 deg.

Table 3 Simulation performed with actuator positions, regulator performance characteristics, and value of degree of controllability

Simulation no.	Actuator positions	Maximum $\Delta\Sigma$, deg	Maximum $\Delta\Theta$, deg	Settling time, s	Controllability $\varepsilon = \infty$
1	No actuators	0.0370	0.02300	12.6	0
2	16, 11	0.0190	0.00783	11.5	1.194
3	16, 10	0.0194	0.00890	11.5	0.891
4	17, 9	0.0220	0.00730	11.7	0.632
5	18, 9	0.0220	0.00790	11.7	0.130
6	19, 9	0.0210	0.00680	11.7	0.507
7	23, 9	0.0194	0.00890	11.8	0.117

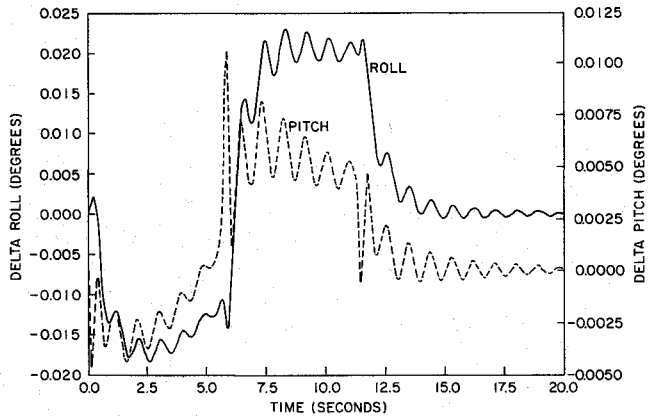

Fig. 3 Flexure in roll and pitch vs time. Simulation no. 1 with no actuators.

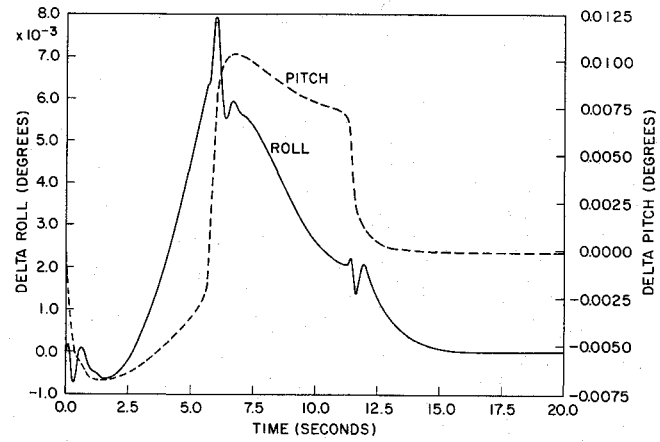

Fig. 4 Flexure in roll and pitch vs time. Simulation no. 2 with maximum value of degree of controllability.

Seven simulations are made with different choices for actuator placements and, therefore, different values of ρ_{ij}; the baseline case with no proof-mass actuators is denoted as simulation 1. The simulation time in the runs is 20 s, which includes 11.30 s (2^*t_s) for the slew maneuver, plus an additional 8.70 s to compute settling performance. Table 3 gives the actuator locations for all seven simulations and the values of 1) maximum Σ, 2) maximum $\Delta\theta$, 3) simulation time when Σ dropped below 0.01 deg, and 4) degree of controllability ρ_{ij} with $\varepsilon = 10$. Figure 3 shows $\Delta\theta$ and $\Delta\phi$ vs time for simulation 1. Figure 4 shows $\Delta\theta$ and $\Delta\phi$ for simulation 2, which gave the best performance in terms of max Σ and settling time. Figure 5 shows $\Delta\theta$ from simulation 2 and from simulation 7 on the same plot for comparison purposes.

In simulation 1, made without the actuators in operation, the jumps in $\Delta\theta$ occur at $t = t_s$ and at $t = 2^*t_s$. An oscillation of about 1.1 Hz appears in both the roll and pitch flexure history. This mode is closest in frequency to the second roll mode, mode 4, which is 1.18 Hz, and seems to couple into the pitch flexure. Modes 1,2, and 3 are damped because they have maxima near the reflector and are controllable by the end thrusters. The modes of order higher than 4 are of amplitude too small to appear in the figures. These modes are either highly damped or not stimulated during the nonlinear slew.

In simulation 2, made with the proof-mass actuators at maximum controllability (for $\varepsilon = \infty$), it can be seen that Σ settles below 0.01 deg at 0.2 s after switchoff, $t = 2^*t_s$. Mode 4 is strongly damped in this simulation. Simulations 2–7 show a reduction of damping with placement of the actuators into positions of reduced controllability. Figure 5 illustrates this decreased damping. It shows that the jumps in $\Delta\theta$ in simulation 2 are more strongly damped than in simulation 7, although the maximum $\Delta\theta$ is greater in simulation 2. The limit of 44.48 N actuator force was not reached for any of the calculations. A smaller value of r than 10^{-7}, for $[R] = r[I]$ of Eq. (12), used in the development of the LQR regulator, would have resulted in larger actuator forces.

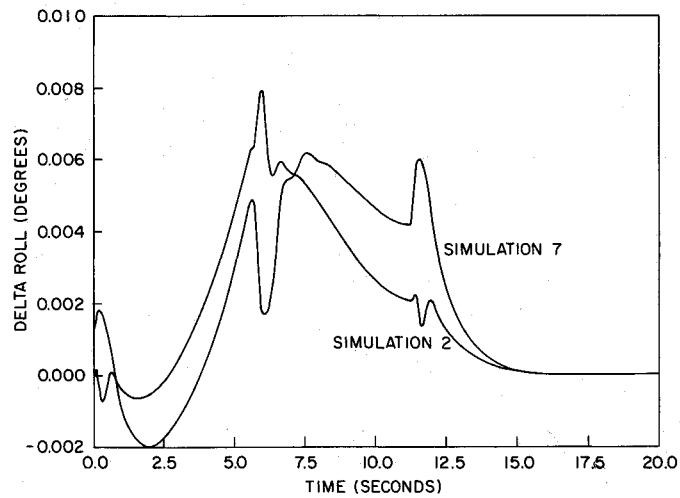

Fig. 5 Flexure in roll vs time. Comparison of simulation no. 2 and simulation no. 7.

Placement Considerations for Actuators: Degree of Controllability

The simulations show a relative insensitivity of damping to changes in actuator placement, provided that the actuators are not located too close to the ends of the beam. The simulations also show that damping is decreased for configurations with actuators close to the ends of the beam. Furthermore, the simulations generally indicate a positive correlation between the

magnitude of the degree of controllability and the amount of damping. The usefulness of such a result is that degree of controllability methods are relatively easy to apply to complex structures, particularly when compared with the alternative of performing a series of simulations.

Design Challenge Considerations: Pointing Accuracy and Slew

The design challenge calls for a pointing accuracy of 0.02 deg of the LOS, after completion of the slew, and settling. In the simulation performed in this analysis, the flexure amplitude settled below 0.01 deg after about 0.2 s after switchoff of the slewing torques. This is a hopeful sign that the goal of a pointing error of less than 0.02 deg can be reached, although consideration must be given to effects not included in this study. Sensor time lag, actuator dynamics, particularly time lag and limited actuator travel distance, noise in the system, and changes in mode shapes due to beam rotation could be important. Gyroscopic stiffening[18,19] was not included, but is not important here since the slew rotation frequency is an order of magnitude less than the lowest modal frequency.

Improvements in LOS pointing accuracy could be achieved by including the effects of changes in the minimum inertia axis during the slew, and by implementation of a closed-loop control law.

The slew could be made faster by "snapping" the beam with a large bend prior to initiating the slew, or by application of the full 3558 N (800 lb) force to the reflector that is allowable in the SCOLE design. Either of the above implementations would generate large bends in the beam, and would require a regulator to treat finite-amplitude flexure.

References

[1]Taylor, L. W. and Balakrishnan, A. V., "A Laboratory Experiment Used to Evaluate Control Laws for Flexible Spacecraft...NASA/IEEE Design Challenge," *Proceedings of the Fourth AIAA/VPI&SU Symposium on Dynamics and Control of Large Structures*, AIAA, New York, 1983, pp. 311–318; revised June 1984.

[2]Williams, J. P. and Rallo, R. A., "Discription of the Spacecraft Control Laboratory Experiment (SCOLE) Facility," NASA Langley Research Center, NASA TM 89057, Jan. 1987.

[3]Taylor, L. W. (ed), *SCOLE Workshop—1986. Proceedings,* NASA TM 80975, Nov. 1986; *SCOLE Workshop—1985, Proceedings,* NASA TM 89048, Dec. 1985; *SCOLE Workshop—1984, Proceedings,* Dec. 1984, NASA Langley Research Center, Hampton, VA.

[4]Quinn, R. D. and Meirovitch, L., "Maneuver and Vibration Control of SCOLE," *Proceedings of the AIAA Guidance, Navigation and Control Conference*, AIAA, New York, 1986, pp. 115–129.

[5]Meirovitch, L. and Quinn, R. D., "Equations of Motion for Maneuvering Flexible Spacecraft," *Journal of Guidance, Control, and Dynamics* (submitted for publication.)

[6]Norris, G. A., Collins, E. G., and Skelton, R. E., "Regulation of the Scole Configuration," *SCOLE Workshop—1986 Proceedings,* NASA TM 89075, 1986, p. 321.

[7]Lin, J. G., "Rapid Torque Limited Line-of-Sight Pointing of SCOLE," *Proceedings of the AIAA Guidance, Navigation and Control Conference*, AIAA, New York, 1986, pp. 106–114.

[8]Kakad, Y. P., "Dynamics and Control of Slew Maneuver of Large, Flexible Spacecraft," *Proceedings of the AIAA Guidance, Navigation and Control Conference*, AIAA, New York, 1986, pp. 629–634.

[9]Kakad, Y. P., "Dynamics of Spacecraft Control Laboratory Experiment (SCOLE) Slew Maneuver," NASA CR 4098, Oct. 1987.

[10]Bainum, P. and Li, F. "Optimal Torque Control for Slewing Maneuvers," *SCOLE Workshop—1986 Proceedings,* NASA TM 89075, 1986 p. 69.

[11]Bodley, C. S., Devers, A. D., Park, A. C., and Frisch, H. P., "A Digital Computer Program for the Dynamic Interaction Simulation of Controls and Structure (DISCOS)," NASA Tech Paper 1219, May 1978.

[12]Schaeffer, H. G., "MSC/NASTRAN Primer, Static and Normal Modes Analysis," Schaeffer Analysis, Inc., Mount Vernon, NH, 1984.

[13]Graig, R. R., *Structural Dynamics, An Introduction to Computer Methods*, Wiley, New York, 1981.

[14]Chodas, J. L. and Macala, G. A., "Validation of the Galileo Scan Platform Control Design Using DISCOS," *Proceedings of the AIAA Astrodynamics Conference,* AIAA, New York, 1984, pp. 681–692.

[15]Lewis, F., *Optimal Control,* Wiley, New York, 1986, p. 254.

[16]Viswanathan, C. N., Longman, R. W., and Likins, P. W., "A Degree of Controllability Definition: Fundamental Concepts and Application to Modal Systems." *Journal of Guidance, Control, and Dynamics*, Vol. 7, March–April 1984, pp. 220–230.

[17]Lindberg, R. E., Jr., "Actuator Placement Considerations for the Control of Large Space Structures," Naval Research Lab., Washington, DC, NRL Rept. 8675, May 1983.

[18]Chun, H. M., "Large-Angle Slewing Maneuvers for Flexible Spacecraft," Ph.D. Dissertation, Dept. of Aeronautics and Astronautics, Massachusetts Inst. of Technology, Cambridge, MA, Sept. 1986, pp. 143–144.

[19]Kane, T. R., Ryan, R. R., and Banerjee, A. K., "Dynamics of a Beam Attached to a Moving Base, AAS Paper 85-390, Aug. 1985